

This article was downloaded by: [Tomsk State University of Control Systems and Radio]

On: 23 February 2013, At: 07:03

Publisher: Taylor & Francis

Informa Ltd Registered in England and Wales Registered Number: 1072954

Registered office: Mortimer House, 37-41 Mortimer Street, London W1T 3JH, UK



Molecular Crystals and Liquid Crystals

Publication details, including instructions for authors and subscription information:

<http://www.tandfonline.com/loi/gmcl16>

Orientalional Effects in Heat-Conducting Nematic Liquid Crystals

M. N. L. Narasimhan^{a b} & A. C. Eringen^a

^a Department of Aerospace and Mechanical Sciences, Princeton University, Princeton, N. J., 08540

^b Oregon State University, Department of Mathematics, Corvallis, Oregon, 97331

Version of record first published: 21 Mar 2007.

To cite this article: M. N. L. Narasimhan & A. C. Eringen (1974): Orientalional Effects in Heat-Conducting Nematic Liquid Crystals, Molecular Crystals and Liquid Crystals, 29:1, 57-87

To link to this article: <http://dx.doi.org/10.1080/15421407408083188>

PLEASE SCROLL DOWN FOR ARTICLE

Full terms and conditions of use: <http://www.tandfonline.com/page/terms-and-conditions>

This article may be used for research, teaching, and private study purposes. Any substantial or systematic reproduction, redistribution, reselling, loan, sub-licensing, systematic supply, or distribution in any form to anyone is expressly forbidden.

The publisher does not give any warranty express or implied or make any representation that the contents will be complete or accurate or up to date. The accuracy of any instructions, formulae, and drug doses should be independently verified with primary sources. The publisher shall not be liable

for any loss, actions, claims, proceedings, demand, or costs or damages whatsoever or howsoever caused arising directly or indirectly in connection with or arising out of the use of this material.

Orientational Effects in Heat-Conducting Nematic Liquid Crystals†

M. N. L. NARASIMHAN‡ and A. C. ERINGEN

Department of Aerospace and Mechanical Sciences, Princeton University, Princeton, N.J. 08540

(Received August 30, 1973; in final form April 8, 1974)

An analysis of mutually competing orienting influences on heat-conducting nematic liquid crystals, of temperature gradients, solid boundaries and shear flows is carried out in the case of Couette flow between concentric rotating cylinders by solving the governing equations on the basis of the micropolar continuum theory of Eringen.¹⁻⁴ Several new features of this investigation distinguishing it from other existing theories include the derivation of explicit analytical expressions for apparent viscosity, adsorption layer, orientation field, microgyration velocity and heat-conduction thus allowing for a direct and more satisfying comparison with experimental results. The behavior of apparent viscosity under various shear-rates and temperatures as well as its dependence on the gap-width between the cylinders is investigated. The theoretical predictions are found to be in good agreement with experimental results.

1 INTRODUCTION

In a companion paper⁵ we have developed a theory of heat-conducting nematic liquid crystals on the basis of the micropolar theory originated by Eringen.¹⁻⁴ It is well known that the nematic liquid crystal is distinguished from other types of liquid crystals in that it possesses certain fundamental symmetries which lead to its invariant properties under spatial reflections. It is also well known from experimental investigations that the molecules of liquid crystals, generally assumed to be rigid and rod-like and parallel to one another, are readily orientable when subjected to electric fields,⁶

† The present work was partially supported by the National Science Foundation.

‡ On leave from Oregon State University, Department of Mathematics, Corvallis, Oregon 97331

magnetic fields,⁷ shear fields,^{8,9} temperature gradients¹⁰ and even by their proximity to solid boundaries.¹¹ Lee and Eringen¹²⁻¹⁴ have established that the nematic liquid crystal, in its natural state has an axis of orientation and in the case of non-heat conducting nematic liquid crystal they have investigated boundary and shear effects as well as magnetic effects on orientation and also have obtained solutions for wave propagation.

The purpose of the present paper is to investigate the mutually competing effects on the orientation of heat-conducting nematic liquid crystals, of temperature gradients, solid boundaries and shear fields. Also it is the purpose to develop here a theoretical analysis which can provide a means for a direct and explicit comparison of our theoretical predictions with available experimental results as well as to obtain a means of determining some of the material coefficients present in the theory. For this purpose, the linear theory derived in Ref. 5 is used.

The effects of temperature gradient on orientation of liquid crystals was first observed by Lehmann.¹⁵ When heating liquid crystals he found, by using a microscope, violent rotations in droplets in the presence of a temperature gradient. Anzelius¹⁶ attempted to analyze this effect of temperature gradient competing with boundary effects. However, his theory did not contain the currently known continuum principles. Oseen¹⁷ criticized the static theory of Anzelius and put forth a dynamic explanation of this phenomenon and concluded that the motion was due to the molecules rotating with uniform speed around vertical axes drawn through their centers of gravity. But his theory lacked the explanation of the forces causing the motion. Leslie¹⁸ using his constitutive theory¹⁹ attempted to explain the rotation in cholesteric liquid crystals (special case of twisted nematics) which led to some controversial questions relating to the thermomechanical coupling involved in the problem. For an account of this we refer the reader to the paper by V. S. V. Rajan and J. J. C. Picot²⁰ and also Leslie's subsequent paper.²¹

Stewart²² was the first one, however, to carry out a systematic experimental observation of temperature gradient effect using X-ray diffraction studies on nematic *p*-azoxyanisole. He concluded that a small temperature gradient of 1° or 2°C/cm produces a preferred orientation of the liquid crystal molecules with their long axes perpendicular to the direction of maximum temperature gradient. The experiments of Picot and Fredrickson,¹⁰ Yun *et al.*,²³ Fisher and Fredrickson,²⁴ Porter and Johnson⁸ show that the heat-conduction effects on orientation do not compete successfully with shear-orientation effects at stresses above a certain minimum. A formal explanation of the observation of Stewart *et al.*²⁵ has been attempted by Davison²⁶ and Davison and Amos²⁷ based on a linear constitutive theory derived along the lines of Ericksen's^{28,29} non-linear constitutive theory for liquid

crystals. Davison²⁶ arrives at the conclusion that the presence of a temperature field affects the orientation field by introducing an intrinsic body moment on the director. If the boundaries also prescribe such moments, the coupling that results complicates Davison's equations particularly with general type of orientations and also where thermal conductivity is anisotropic. The difference between the present work and Davison's work lies in the different constitutive theories applied. While Davison's work follows Ericksen's^{28,29} constitutive theory, the present work is based on Eringen's theory¹⁻⁴ and also our theory developed in Ref. 5. Since Eringen³⁰ has already explained very clearly the vital difference between his theory and Ericksen's theory, we do not repeat those details again here. Moreover, the present work is concerned with Couette flow of heat-conducting nematic liquid crystals while Davison's work²⁶ is concerned with applications to wave propagation problems involving splay, bending and twist waves.

Hence, it seems evident that a deeper and detailed research is needed to study the anisotropic effects of heat-conduction competing with boundary and shear effects on orientation of heat-conducting nematic liquid crystals. With this view in mind, the present work was undertaken using the linear thermomicropolar theory derived in Ref. 5. We therefore consider Couette flow of heat-conducting nematic liquid crystals since most of the experiments are conducted in either Couette viscometers or capillary tubes. Atkin and Leslie³¹ have investigated Couette flow and Atkin³² has discussed Poiseuille flow of nematic liquid crystals. Their analysis neglects heat-conduction altogether. On the other hand, there is evidence to believe (as shown later in the present work) that there clearly exists a contribution to heat-conduction due to the micropolar nature of the flow whether or not an externally imposed temperature gradient is present. This appears to be one of the new predictions of the micropolar theory. Any analysis would therefore be incomplete without taking into account the presence of such micropolar heat-conduction effects. Moreover, Atkin and Leslie's work³¹ being highly non-linear does not seem to permit linearization without losing its relevance to liquid crystals and the various material coefficients involved in their constitutive theory do not correspond to the existing experimental measurements. Consequently their theory does not lend itself to direct comparison of their results with available experimental measurements. This defect is remedied in the present work based on the thermomicropolar theory developed in Ref. 5 which readily lends itself to the derivation of a linear theory without losing its relevance to liquid crystals thus allowing for a direct and close comparison of our theoretical predictions with experimental data. Indeed the micropolar theory yields explicit analytical expressions for orientation field, apparent viscosity and heat-conduction. The phenomenon of formation of adsorption layers at the walls of the cylinders has been adequately accounted for in our

investigation. The mutually competing effects on the orientation, of temperature gradients, solid boundaries and shear flows have been investigated. The behavior of apparent viscosity under varying rates of shear throughout the nematic temperature range in the case of the nematic *p*-azoxyanisole has been analytically obtained and is compared with the experimentally observed behavior obtaining a good agreement. It is found that apparent viscosity decreases with increasing shear-rate at a given temperature and approaches a constant limit for shear-rates above $2 \times 10^3 \text{ sec}^{-1}$, while for narrow gap width of the order of 10^{-3} mm between the cylinders higher values of the viscosity are obtained for the same range of shear-rates. For decreasing shear-rates at a given temperature within the nematic range, however, the viscosity is found to increase, highest values of viscosity occurring at lowest possible rates of shear. These predictions of our theory are found to be in good agreement both qualitatively and quantitatively with the experimental results of Porter and Johnson,⁸ Peter and Peters,³³ Becherer and Kast³⁴ and Miesowicz.³⁵ Furthermore, this comparison of our theory with the above mentioned experimental results and also other existing theories such as those of Frank³⁶ leads to the actual determination of at least some of the material coefficients present in the micropolar constitutive theory of heat-conducting liquid crystals.

2 BASIC EQUATIONS

We recall that the equations of motion of a general micropolar continuum^{1,3,4,13} and constitutive equations for heat-conducting anisotropic nematic liquid crystals obtained in Ref. 5 reduce in the linear incompressible case to the following:

$$v_{k,k} = 0, \quad (2.1)$$

$$\frac{\partial i_{kl}}{\partial t} + i_{kl,m} v_m + e_{lmr} v_r i_{km} + e_{kmr} v_r i_{ml} = 0, \quad (2.2)$$

$$t_{ji,j} + \rho(f_i - \dot{v}_i) = 0, \quad (2.3)$$

$$m_{ji,j} + e_{ikl} t_{kl} + \rho(l_i - \dot{\sigma}_i) = 0, \quad (2.4)$$

$$\rho \dot{e} = t_{kl}(v_{l,k} - e_{klm} v_m) + m_{kl} v_{l,k} + q_{k,k} + \rho h, \quad (2.5)$$

$$t_{kl} = -p \delta_{kl} + a_{klmn}(v_{n,m} - e_{mnp} v_p), \quad (2.6)$$

$$m_{kl} = B_{ikmn} \phi_{m,n} + b_{ikmn} v_{m,n} + \gamma_{ikmn} g_{mn}, \quad (2.7)$$

$$q_b = (d_{ikmn} v_{m,n} + \delta_{ikmn} g_{mn}) \frac{1}{2} e_{lkb}, \quad (2.8)$$

$$\begin{aligned} \psi &= \varepsilon - T\eta = \psi(\rho^{-1}, T, \phi_{m,n}) \\ &= \psi_0(\rho^{-1}, T) + (\frac{1}{2}\rho) B_{klmn}(\rho^{-1}, T) \phi_{k,l} \phi_{m,n} \end{aligned} \quad (2.9)$$

where t_{ij} , m_{ij} , q_b are respectively the stress tensor, the moment stress tensor and the heat-flux vector, f_i is the body force, v_i is the velocity vector, p is the pressure to be determined by the equations of motion, ε is the internal energy density per unit mass, h is the heat supply per unit mass, l_i is the body couple, ρ is the mass density, $v_k = \dot{\phi}_k$ is the microgyration velocity vector, $\dot{\phi}_m$ is the angular microrotation vector and g_{mn} given by

$$g_{mn} = \frac{1}{2} T^{-1} e_{mnq} T, \quad (2.10)$$

is the temperature gradient bivector, T is the temperature, e_{mnq} is the alternating tensor and the spin-inertia $\dot{\sigma}_i$ is given by

$$\dot{\sigma}_i = (i_{mm} \delta_{ij} - i_{ij}) \dot{v}_j - e_{kij} i_{km} v_m v_j, \quad (2.11)$$

in which $i_{kl} = i_{lk}$ is the micro-inertia tensor which satisfies the conservation law, (2.2),¹³ δ_{ij} is the kronecker delta, and $\psi = \varepsilon - T\eta =$ Helmholtz free energy density, η being the specific entropy. The constitutive Eq. (2.9) for ε , was obtained by Eringen,¹³ while deriving a linear constitutive theory for nematic liquid crystals. Furthermore, in Ref. 5, we have obtained the generalized Clausius–Duhem inequality and also the thermodynamic restrictions governing the constitutive equations and hence we will not repeat them here.

Throughout this paper we employ spatial and material rectangular coordinate systems x_i , ($i = 1, 2, 3$), and X_I , ($I = 1, 2, 3$) and assume summation convention over repeated indices. An index followed by a comma represents partial differentiation with respect to the space variable, and a superposed dot indicates material differentiation, e.g.,

$$v_{k,l} = \partial v_k / \partial x_l, \quad x_{k,K} = \partial x_k / \partial X_K, \quad \dot{v}_k = \partial v_k / \partial t + v_{k,l} v_l.$$

The coefficients a_{klmn} are given by

$$a_{klmn} = a_{KLMN} \delta_{kK} \delta_{lL} \delta_{mM} \delta_{nN}, \quad (2.12)$$

are functions of temperature only, δ_{kK} being the direction cosines between the spatial and material coordinates. Similar statements as (2.12) hold for the coefficients b_{klmn} , d_{klmn} , B_{klmn} , γ_{klmn} and δ_{klmn} also. Thermodynamic and material symmetry restrictions on these material moduli are given in the companion paper.⁵ The motion of a material point X_K is given by $x_k = x_k(X_K, t)$ and χ_{kK} is the micromotion.

3 FORMULATION OF THE PROBLEM

We consider a steady Couette flow of heat-conducting nematic liquid crystals, between two long concentric circular cylinders of radii r_1 and r_2 ($r_1 < r_2$) which are rotating with constant angular velocities Ω_1 and Ω_2 , respectively.

Cylindrical polar coordinates (r, θ, z) are chosen such that the z -axis, coincides with the common axis of the cylinders. Let (x, y, z) and (X, Y, Z) represent spatial and material rectangular coordinates. We assume that these spatial and material frames are coincident and hence in view of (2.12) the coefficients a_{klmn} , etc., become the actual material coefficients. We choose the material frame in such a way that the X -axis coincides with the axis of orientation of the liquid crystal. The velocity field and the microgyration velocity field are respectively, given by

$$v_r = 0, \quad v_\theta = r\omega(r, \theta), \quad v_z = 0, \quad (3.1)$$

$$v_r = 0, \quad v_\theta = 0, \quad v_z = v(r, \theta). \quad (3.2)$$

Since the velocity components have to satisfy the equation of continuity for the present incompressible case $v_{k,k} = 0$, it follows that ω must be a function of r only, $\omega = \omega(r)$. The temperature field is $T = T(r)$. We allow arbitrary spatial dependence for v to depend on both r and θ , consequently, as we shall see later, the pressure field is also dependent on both r and θ (since all quantities are independent of the z -coordinate) in order to provide the inner structure with additional degrees of freedom.

The micromotion is given by

$$(\chi_{kK}) = \begin{pmatrix} \cos \phi & -\sin \phi & 0 \\ \sin \phi & \cos \phi & 0 \\ 0 & 0 & 1 \end{pmatrix} \quad (3.3)$$

where

$$\phi = (0, 0, \phi(r, \theta)), \quad (3.4)$$

is the orientation vector, ϕ being the angle between the long axis of a molecule of the liquid crystal and the axis of orientation. In cartesian coordinates, (3.1) and (3.2) become

$$v_x = -r\omega(r)\sin \theta, \quad v_y = r\omega(r)\cos \theta, \quad v_z = 0, \quad (3.5)$$

$$v_x = 0 = v_y, \quad v_z = \dot{\phi} = v(r, \theta). \quad (3.6)$$

It has been shown⁵ that the use of full material symmetry of the nematic liquid crystal, such as the *p*-azoxyanisole, leads to the following non-vanishing components of the material moduli a_{klmn} :

$$\begin{aligned} a_{1111} &= a_{2222}, a_{1122} = a_{2211}, a_{1133} = a_{2233}, a_{3311} = a_{3322}, a_{3333}, \\ a_{1313} &= a_{2323}, a_{1331} = a_{2332}, a_{3113} = a_{3223}, a_{3131} = a_{3232}, \\ a_{1212} &= a_{2121}, a_{1221} = a_{2112} = a_{1111} - a_{1122} - a_{1212}, \end{aligned}$$

with similar statements for other material coefficients

$$b_{klmn}, d_{klmn}, B_{klmn}, \gamma_{klmn} \text{ and } \delta_{klmn} \text{ also.}$$

Substitution of (3.4), (3.5) and (3.6) into Eqs. (2.6) to (2.8) yields the following:
The stress components are:

$$\begin{aligned}
 t_{xx} &= t_{11} = -p - k_1 r \omega' \sin 2\theta, \\
 t_{yy} &= t_{22} = -p + k_1 r \omega' \sin 2\theta, \\
 t_{zz} &= t_{33} = -p, \\
 t_{xy} &= t_{12} = r \omega' (k_3 + k_1 \cos 2\theta) + 2k_3(\omega - v), \\
 t_{yx} &= t_{21} = -[r \omega' (k_3 - k_1 \cos 2\theta) + 2k_3(\omega - v)], \\
 t_{xz} &= 0 = t_{zx} = t_{yz} = t_{zy};
 \end{aligned} \tag{3.7}$$

The moment-stress components are:

$$\begin{aligned}
 m_{xx} &= m_{11} = 0, m_{yy} = m_{22} = 0, m_{zz} = m_{33} = 0, m_{xy} = m_{12} = 0, \\
 m_{yx} &= m_{21} = 0, m_{zx} = m_{31} = k_5 \phi_{,x} + k_6 v_{,x} + k_7 T_{,y}, \\
 m_{xz} &= m_{13} = k_8 \phi_{,x} + k_9 v_{,x} + k_{10} T_{,y}, \\
 m_{zy} &= m_{32} = k_5 \phi_{,y} + k_6 v_{,y} - k_7 T_{,x}, \\
 m_{yz} &= m_{23} = k_8 \phi_{,y} + k_9 v_{,y} - k_{10} T_{,x}.
 \end{aligned} \tag{3.8}$$

The heat-flux vector components are:

$$q_x = q_1 = k_{11} v_{,y} + k_{12} T_{,x}, q_y = q_2 = -k_{11} v_{,x} + k_{12} T_{,y}, q_z = q_3 = 0, \tag{3.9}$$

where

$$\begin{aligned}
 k_1 &= \frac{1}{2}(a_{1111} - a_{1122}) = k_4, k_2 = a_{3311}, k_3 = \frac{1}{2}(a_{1212} - a_{1221}), \\
 k_5 &= B_{1331}, k_6 = b_{1331}, k_7 = \frac{1}{2}T^{-1}(\gamma_{1331} - \gamma_{1313}), k_8 = B_{3131}, \\
 k_9 &= b_{3131}, k_{10} = \frac{1}{2}T^{-1}(\gamma_{3131} - \gamma_{3113}), k_{11} = \frac{1}{2}(d_{2332} - d_{3232}), \\
 k_{12} &= \frac{1}{4}T^{-1}(\delta_{2323} - \delta_{3223} - \delta_{2332} + \delta_{3232}),
 \end{aligned} \tag{3.10}$$

are functions of temperature only and the prime denotes differentiation with respect to r .

After substituting Eqs. (3.7) to (3.9) into the balance equations of motion and energy, (2.3) to (2.5), we obtain the final field equations governing $\omega(r)$, $p(r, \theta)$, $T(r)$ and $v(r, \theta)$ (in the absence of external body forces, body couples, and heat sources):

$$k(r\omega'' + 3\omega') - \left(\frac{\partial v}{\partial r} + \alpha \frac{\partial p}{r\partial\theta}\right) - \left(\frac{\partial v}{r\partial\theta} - \alpha \frac{\partial p}{\partial r}\right)\cot\theta = 0, \tag{3.11}$$

$$k(r\omega'' + 3\omega') - \left(\frac{\partial v}{\partial r} + \alpha \frac{\partial p}{r\partial\theta}\right) + \left(\frac{\partial v}{r\partial\theta} - \alpha \frac{\partial p}{\partial r}\right)\tan\theta = 0, \tag{3.12}$$

$$B_{3131}\nabla^2\phi + b_{3131}\nabla^2v + \frac{1}{\alpha}(r\omega' + 2\omega) - \frac{2}{\alpha}v - \rho j\dot{v} = 0, \tag{3.13}$$

$$\nabla^2 T = 0, \tag{3.14}$$

where

$$\alpha = (a_{1212} - a_{1221})^{-1}, j = i_{11} + i_{22}, k = \alpha a_{1212}, \quad (3.15)$$

$$\nabla^2 = \frac{\partial^2}{\partial r^2} + \frac{1}{r} \frac{\partial}{\partial r} + \frac{1}{r^2} \frac{\partial^2}{\partial \theta^2}. \quad (3.16)$$

In order that a solution set for (3.11) to (3.14) may exist under appropriate boundary conditions, in view of (3.15)₁, we must have

$$a_{1212} - a_{1221} \neq 0, \quad (3.17)$$

which is readily permitted by the thermodynamic restrictions on a_{1212} and a_{1221} already obtained in Ref. 5, namely,

$$a_{1212} \geq 0, a_{1212} - a_{1221} \geq 0 \quad (3.18)$$

Hence, for a solution set to exist for the field equations, in view of (3.17) and (3.18), we must have, $a_{1212} - a_{1221} > 0$.

In addition, we note from the thermodynamic restrictions obtained in Ref. 5, that the material coefficient B_{3131} is not subject to thermodynamic restrictions. Hence, if we are seeking an explicit solution for the orientation field ϕ , we must assume that $B_{3131} \neq 0$, for otherwise, the term involving ϕ in (3.13) would be completely eliminated and no other equation in the set contains ϕ explicitly. Hence we seek a solution set for the Eqs. (3.11) to (3.14) under appropriate boundary conditions when

$$a_{1212} - a_{1221} > 0, B_{3131} \neq 0. \quad (3.19)$$

Thus α and hence k defined in (3.15) are bounded and positive. We recall that a dot on a variable denotes material derivative. In the steady state case, we have

$$\frac{D}{Dt} = \omega(r) \frac{\partial}{\partial \theta} = \omega \frac{\partial}{\partial \theta}, v = \frac{D\phi(r, \theta)}{Dt} = \omega \frac{\partial \phi}{\partial \theta}, \dot{v} = \omega \frac{\partial v}{\partial \theta} \approx 0, \quad (3.20)$$

the last of the equations, (3.20)₃ follows since we consider the linear case where both ω and v are small.

The term $\rho j v$ in Eq. (3.13) is of second order smallness since from Eq. (3.20), $\dot{v} \approx 0$ and hence can be neglected in comparison with the rest of the terms which are of the first order.

In the linear micropolar theory, the term $\rho \dot{\epsilon}$ on the left-hand side of the energy Eq. (2.5) consists of only second order terms in view of the fact that $\dot{v} \approx 0$ and $\dot{T} = \omega(\partial/\partial\theta)(T(r)) = 0$ from (3.20) and from (2.9), $\eta = -\partial\psi/\partial T$. Thus we have from (2.9), in the linear theory,

$$\rho \dot{\epsilon} = \rho(\dot{\psi} + \dot{\eta}T + \eta\dot{T}) \approx \rho\dot{\psi}_0(\rho^{-1}, T) + \rho\dot{\eta}T = 0.$$

Since, in the linear theory,

$$\begin{aligned}\dot{\psi} &= \dot{\psi}_0(\rho^{-1}, T) + \text{higher order terms} \simeq \dot{\psi}_0(\rho^{-1}, T) \\ &= \omega \frac{\partial}{\partial \theta} [\psi_0(\rho^{-1}, T(r))] = 0\end{aligned}$$

and

$$\dot{\eta} = \frac{D}{Dt} \left(-\frac{\partial \psi}{\partial T} \right) \simeq \omega \frac{\partial}{\partial \theta} [\psi_0(\rho^{-1}, T(r))] + \text{higher order terms} \simeq 0.$$

On the right-hand side of (2.5), all terms except the term $q_{k,k}$ are second-order terms and hence can be neglected in comparison with the first-order small terms ω , v and ∇T in the linear theory and the heat source term $h = 0$. Thus, (2.5) reduces to $q_{k,k} = 0$ which by virtue of (3.9) becomes Eq. (3.14).

4 METHOD OF SOLUTION AND DISCUSSION OF BOUNDARY CONDITIONS

We shall now examine under what type of boundary conditions a physically realizable solution exists for the system (3.11) to (3.14). Writing

$$k(r\omega'' + 3\omega') = f(r), \frac{\partial v}{\partial r} + \alpha \frac{\partial p}{r\partial \theta} = g(r, \theta), \frac{\partial v}{r\partial \theta} - \alpha \frac{\partial p}{\partial r} = h(r, \theta), \quad (4.1)$$

and taking the material time-derivative of Eq. (3.13), Eqs. (3.11) to (3.14) become, since $B_{3131} \neq 0$ and $\omega(r) \neq 0$,

$$f(r) - g(r, \theta) - h(r, \theta)\cot \theta = 0, \quad (4.2)$$

$$f(r) - g(r, \theta) + h(r, \theta)\cot \theta = 0, \quad (4.3)$$

$$\frac{\partial}{\partial \theta} (\nabla^2 \phi) = 0, \quad (4.4)$$

$$\nabla^2 T = 0. \quad (4.5)$$

It readily follows from (4.2) and (4.3) that $h(r, \theta) = 0$, and hence we have

$$f(r) = g(r, \theta) = g(r). \quad (4.6)$$

Consequently, from (4.1) we have

$$k(r\omega'' + 3\omega') = \frac{\partial v}{\partial r} + \alpha \frac{\partial p}{r\partial \theta}, \quad (4.7)$$

$$\frac{\partial v}{\partial \theta} = \alpha r \frac{\partial p}{\partial r}. \quad (4.8)$$

Elimination of v from (4.7) and (4.8) yields

$$\nabla^2 p = \frac{\partial^2 p}{\partial r^2} + \frac{1}{r} \frac{\partial p}{\partial r} + \frac{1}{r^2} \frac{\partial^2 p}{\partial \theta^2} = 0. \quad (4.9)$$

whose general solution is of the form

$$\begin{aligned} p(r, \theta) = & p_0 + c_0 \ln r + \sum_{n=1}^{\infty} r^n (p_n \cos n\theta + q_n \sin n\theta) \\ & + \sum_{n=1}^{\infty} r^{-n} (s_n \cos n\theta + t_n \sin n\theta), \end{aligned} \quad (4.10)$$

where c_0, p_0, p_n 's, q_n 's, s_n 's and t_n 's are the Fourier coefficients which are to be determined by using appropriate boundary conditions. Substitution of (4.10) into (4.8) and integration with respect to θ , and the requirement that $v(r, \theta)$ be a single-valued function of θ , yield $c_0 = 0$ and hence we obtain

$$\begin{aligned} v(r, \theta) = F(r) - \alpha \left[\sum_{n=1}^{\infty} r^n (q_n \cos n\theta - p_n \sin n\theta) \right. \\ \left. - \sum_{n=1}^{\infty} r^{-n} (t_n \cos n\theta - s_n \sin n\theta) \right], \end{aligned} \quad (4.11)$$

where $F(r)$ is an arbitrary function to be determined later. Since $c_0 = 0$, (4.10) becomes

$$p(r, \theta) = p_0 + \sum_{n=1}^{\infty} r^n (p_n \cos n\theta + q_n \sin n\theta) + \sum_{n=1}^{\infty} r^{-n} (s_n \cos n\theta + t_n \sin n\theta). \quad (4.12)$$

Substituting (4.11) and (4.12) for v and p in (4.1)₂ and equating the result to (4.1)₁, in view of (4.6), we obtain after integrating with respect to r ,

$$F(r) = k(r\omega' + 2\omega) + d, \quad (4.13)$$

where d = constant of integration.

Similarly, the general solution of Eq. (4.4) has the form (after requiring that ϕ should be a single-valued function of θ)

$$\frac{\partial \phi}{\partial \theta} = \sum_{n=1}^{\infty} r^n (a_n \cos n\theta + b_n \sin n\theta) + \sum_{n=1}^{\infty} r^{-n} (c_n \cos n\theta + d_n \sin n\theta). \quad (4.14)$$

Substitution of (4.14) into (3.20)₂, yields another alternate expression for $v(r, \theta)$:

$$v(r, \theta) = \omega \frac{\partial \phi}{\partial \theta} = \omega(r) \left[\sum_{n=1}^{\infty} r^n (a_n \cos n\theta + b_n \sin n\theta) + \sum_{n=1}^{\infty} r^{-n} (c_n \cos n\theta + d_n \sin n\theta) \right]. \quad (4.15)$$

That the two expressions for $v(r, \theta)$ given by (4.11) and (4.15) must be equal enables us to determine the unknown function $F(r)$ which appears in (4.11). But, before determining $F(r)$, we discuss the possible boundary conditions under which the solution of the system exists.

The boundary conditions on the velocity field are assumed to be the usual no-slip conditions,

$$\omega(r_1) = \Omega_1, \omega(r_2) = \Omega_2. \quad (4.16)$$

The boundary conditions on $v(r, \theta)$ are some functions of θ on the cylinder walls which may be formally written as

$$v(r_1, \theta) = v_1(\theta), v(r_2, \theta) = v_2(\theta). \quad (4.17)$$

Then, we can evaluate the Fourier coefficients p_n 's, q_n 's, s_n 's and t_n 's in (4.11) and a_n 's, b_n 's, c_n 's and d_n 's in (4.15) in terms of $v_1(\theta)$, $v_2(\theta)$, Ω_1 and Ω_2 . We obtain, when $\Omega_1 \neq 0$, $\Omega_2 \neq 0$ and $R \neq 1$, (the special cases of $\Omega_1 = 0$ or $\Omega_2 = 0$, are considered later in the paper):

$$\begin{aligned} p_n &= U_n(L_n - K_n R^n), q_n = -U_n(N_n - M_n R^n), \\ s_n &= U_n r_1^n r_2^n (L_n R^n - K_n), t_n = -U_n r_1^n r_2^n (N_n R^n - M_n), \\ a_n &= \frac{\alpha U_n}{\Omega_2} (N_n - M_n R^n \Omega_0), b_n = \frac{\alpha U_n}{\Omega_2} (L_n - K_n R^n \Omega_0), \\ c_n &= \frac{\alpha}{\Omega_2} U_n r_1^n r_2^n (M_n \Omega_0 - N_n R^n), d_n = \frac{\alpha}{\Omega_2} U_n r_1^n r_2^n (K_n \Omega_0 - L_n R^n), \end{aligned} \quad (4.18)$$

where

$$\begin{aligned} U_n &= r_2^{-n} (1 - R^{2n})^{-1}, K_n = \frac{1}{\alpha \pi} \int_0^{2\pi} v_1(\theta) \sin n\theta \, d\theta, \\ L_n &= \frac{1}{\alpha \pi} \int_0^{2\pi} v_2(\theta) \sin n\theta \, d\theta, M_n = \frac{1}{\alpha \pi} \int_0^{2\pi} v_1(\theta) \cos n\theta \, d\theta, \\ N_n &= \frac{1}{\alpha \pi} \int_0^{2\pi} v_2(\theta) \cos n\theta \, d\theta, R = \frac{r_1}{r_2}, \Omega_0 = \frac{\Omega_2}{\Omega_1}, \end{aligned} \quad (4.19)$$

and n takes the values $n = 1, 2, 3, \dots, \infty$.

Equating the expressions for $v(r, \theta)$ from (4.11) and (4.15) leads to the following relation:

$$k(r\omega' + 2\omega) + d - \sum_{n=1}^{\infty} [\{\omega(a_n r^n + c_n r^{-n}) + \alpha(q_n r^n - t_n r^{-n})\} \cos n\theta + \{\omega(b_n r^n + d_n r^{-n}) - \alpha(p_n r^n - s_n r^{-n})\} \sin n\theta] \equiv 0. \quad (4.20)$$

An inspection of (4.20) and the expansion of the expression $F(r) = k(r\omega' + 2\omega) + d$ into a Fourier series form corresponding to the second term on the left-hand side of (4.20) leads to the following result:

$$F(r) = k(r\omega' + 2\omega) + d = \sum_{n=0}^{\infty} [A_n(r) \cos n\theta + B_n(r) \sin n\theta],$$

where the Fourier coefficients

$$A_n(r) = \frac{1}{\pi} \int_0^{2\pi} F(r) \cos n\theta \, d\theta = 0; \quad B_n(r) = \frac{1}{\pi} \int_0^{2\pi} F(r) \sin n\theta \, d\theta = 0.$$

Thus we obtain

$$F(r) = k(r\omega' + 2\omega) + d = 0. \quad (4.21)$$

Now, in order that (4.20) which now reduces to

$$\sum_{n=1}^{\infty} [\{\omega(a_n r^n + c_n r^{-n}) + \alpha(q_n r^n - t_n r^{-n})\} \cos n\theta + \{\omega(b_n r^n + d_n r^{-n}) - \alpha(p_n r^n - s_n r^{-n})\} \sin n\theta] \equiv 0,$$

may be satisfied for all arbitrary $\theta \in [0, 2\pi]$ and arbitrary $r \in [r_1, r_2]$, we must have the coefficients of $\cos n\theta$ and $\sin n\theta$ separately vanish. Thus we obtain

$$\omega(a_n r^n + c_n r^{-n}) + \alpha(q_n r^n - t_n r^{-n}) = 0, \quad (4.22)$$

$$\omega(b_n r^n + d_n r^{-n}) - \alpha(p_n r^n - s_n r^{-n}) = 0. \quad (4.23)$$

The solution of (4.21) subject to the boundary conditions (4.16) is:

$$\omega(r) = \frac{\Omega_2 r_2^2 - \Omega_1 r_1^2}{r_2^2 - r_1^2} + \frac{(\Omega_1 - \Omega_2) r_1^2 r_2^2}{r_2^2 - r_1^2} \frac{1}{r^2}, \quad (4.24)$$

which is identical with the classical Couette flow solution.

From (4.22) and (4.23), we have

$$\omega(r) = \frac{-\alpha(q_n r^n - t_n r^{-n})}{(a_n r^n + c_n r^{-n})} = \frac{\alpha(p_n r^n - s_n r^{-n})}{(b_n r^n + d_n r^{-n})}. \quad (4.25)$$

In order that (4.25) may be of the form (4.24) we must have the following relations:

$$\begin{aligned} c_n &= 0 = d_n, \quad \text{for all } n, \\ a_n &= b_n = q_n = t_n = p_n = s_n = 0, \quad \text{for } n > 1. \end{aligned} \quad (4.26)$$

This implies that the only non-vanishing Fourier coefficients in (4.18) occur when $n = 1$ and are a_1, b_1, p_1, q_1, s_1 and t_1 . Furthermore, we have from (4.24) and (4.25),

$$\frac{p_1}{s_1} = \frac{q_1}{t_1} = \frac{\Omega_2 r_2^2 - \Omega_1 r_1^2}{(\Omega_2 - \Omega_1) r_1^2 r_2^2}$$

Substituting (4.18) and (4.19) into (4.27), we obtain the relation to be satisfied by the functions $v_1(\theta)$ and $v_2(\theta)$:

$$\begin{aligned} & \left\{ \int_0^{2\pi} (v_2 - Rv_1) \cos \theta \, d\theta \right\} / \left\{ \int_0^{2\pi} (Rv_2 - v_1) \cos \theta \, d\theta \right\} \\ & \equiv \left\{ \int_0^{2\pi} (v_2 - Rv_1) \sin \theta \, d\theta \right\} / \left\{ \int_0^{2\pi} (Rv_2 - v_1) \sin \theta \, d\theta \right\} \quad (4.28) \\ & \equiv (\Omega_2 r_2^2 - \Omega_1 r_1^2) / (\Omega_2 - \Omega_1) r_1 r_2. \end{aligned}$$

Equation (4.28) is equivalent to:

$$\int_0^{2\pi} (v_2 - Rv_1) \cos \theta \, d\theta \equiv \left[\frac{\Omega_0 - R^2}{(\Omega_0 - 1)R} \right] \int_0^{2\pi} (Rv_2 - v_1) \cos \theta \, d\theta \quad (4.29)$$

and a similar equation with $\cos \theta$ replaced by $\sin \theta$ in (4.29) where

$$R = r_1/r_2, \quad \Omega_0 = \Omega_2/\Omega_1, \quad v_1 = v_1(\theta), \quad \text{and} \quad v_2 = v_2(\theta).$$

From (4.29), we have, after combining the integrals and rearranging them,

$$\int_0^{2\pi} \left(\frac{R}{\Omega_0} v_2 - v_1 \right) \cos \theta \, d\theta \equiv 0 \equiv \int_0^{2\pi} \left(\frac{R}{\Omega_0} v_2 - v_1 \right) \sin \theta \, d\theta. \quad (4.30)$$

In order that (4.30) may be identically satisfied for all choices of the boundary functions $v_1(\theta)$ and $v_2(\theta)$, we must have, clearly,

$$v_2 = \frac{\Omega_0}{R} v_1. \quad (4.31)$$

Now substituting (4.21) into (4.11) and using (4.26) and (4.27) we obtain

$$\begin{aligned} v(r, \theta) &= \frac{\alpha}{r} \left[1 - \left(\frac{\Omega_0 - R^2}{\Omega_0 - 1} \right) \left(\frac{r}{r_1} \right)^2 \right] (t_1 \cos \theta - s_1 \sin \theta) \\ &= a(r) \cos \theta + b(r) \sin \theta, \end{aligned} \quad (4.32)$$

where

$$\begin{aligned} a(r) &= \frac{\alpha}{r} \left[1 - \left(\frac{\Omega_0 - R^2}{\Omega_0 - 1} \right) \left(\frac{r}{r_1} \right)^2 \right] t_1, \\ b(r) &= -\frac{\alpha}{r} \left[1 - \left(\frac{\Omega_0 - R^2}{\Omega_0 - 1} \right) \left(\frac{r}{r_1} \right)^2 \right] s_1, \end{aligned} \quad (4.33)$$

where t_1 and s_1 are to be determined later. Now by the use of (4.17) and (4.31), (4.32) yields the only possible non-trivial forms for $v_1(\theta)$ and $v_2(\theta)$:

$$\begin{aligned} v(r_1, \theta) &= v_1(\theta) = a \cos \theta + b \sin \theta \\ v(r_2, \theta) &= v_2(\theta) = \frac{\Omega_0}{R} (a \cos \theta + b \sin \theta). \end{aligned} \quad (4.34)$$

Thus the Couette flow under consideration, described by $\omega(r)$, $v(r, \theta)$ and $p(r, \theta)$ is possible only under the boundary conditions (4.16) and (4.34); otherwise, the motion $\omega(r)$ would have to be only a rigid body rotation, which is excluded from our problem. This leads to the values of a_1 , b_1 , p_1 , q_1 , s_1 , and t_1 to be given by:

$$\begin{aligned} a_1 &= \frac{a}{r_1 \Omega_1}, & b_1 &= \frac{b}{r_1 \Omega_1}, & p_1 &= \frac{b(\Omega_0 - R^2)}{\alpha r_1 (1 - R^2)}, \\ q_1 &= \frac{-a(\Omega_0 - R^2)}{\alpha r_1 (1 - R^2)}, & s_1 &= \frac{b r_1 (\Omega_0 - 1)}{\alpha (1 - R^2)}, & t_1 &= \frac{-a r_1 (\Omega_0 - 1)}{\alpha (1 - R^2)}, \end{aligned} \quad (4.35)$$

and all other a_n , b_n , c_n , d_n , p_n , q_n , s_n and t_n vanish.

The microgyration velocity and pressure field can now be obtained by using the known solution for the velocity field (4.24), in the expressions (4.12) and (4.15) and the boundary conditions (4.34). The temperature field $T(r)$ is obtained by solving Eq. (4.5) subject to the boundary conditions

$$T(r_1) = T_1, \quad T(r_2) = T_2. \quad (4.36)$$

Heat-conduction can be obtained from Eqs. (3.9) by using the known solutions for $v(r, \theta)$ and $T(r)$. Finally the solution set of the governing field equations can be expressed in non-dimensional form, for the case $\Omega_1 \neq 0$, $a \neq 0$, $b \neq 0$ and $R \neq 1$:

$$\begin{aligned} \bar{\omega} &= \frac{\omega(r)}{\Omega_1} = \frac{1}{1 - R^2} \left(\Omega_0 - R^2 + \frac{1 - \Omega_0}{\lambda^2} \right), \\ \bar{v} &= \frac{v(r, \theta)}{b} = \frac{\lambda}{1 - R^2} \left(\Omega_0 - R^2 + \frac{1 - \Omega_0}{\lambda^2} \right) (\sigma \cos \theta + \sin \theta), \end{aligned}$$

$$\bar{p} = \frac{p(r, \theta) - p(r_2, 0)}{P} = \frac{\lambda}{1 - R^2} \left(\frac{\Omega_0 - R^2}{\Omega_0 - 1} + \frac{1}{\lambda^2} \right) (\cos \theta - \sigma \sin \theta) - \frac{1}{R(1 - R^2)} \left(\frac{\Omega_0 - R^2}{\Omega_0 - 1} + R^2 \right), \quad (4.37)$$

$$\bar{T} = \frac{T(r)}{T_1} = \frac{(1 - \kappa) \ln \lambda + \ln R}{\ln R}$$

$$\bar{q}_\lambda = \frac{q_r}{q_0} = \frac{1}{1 - R^2} \left(\Omega_0 - R^2 + \frac{1 - \Omega_0}{\lambda^2} \right) (\cos \theta - \sigma \sin \theta) + \frac{\mu(1 - \kappa)}{\lambda \ln R},$$

$$\bar{q}_\theta = \frac{q_\theta}{q_0} = \frac{-1}{1 - R^2} \left[\Omega_0 - R^2 - \frac{(1 - \Omega_0)}{\lambda^2} \right] (\sigma \cos \theta + \sin \theta),$$

$$\bar{q}_z = 0.$$

Where

$$\begin{aligned} R &= r_1/r_2, \Omega_0 = \Omega_2/\Omega_1, \lambda = r/r_1, \sigma = a/b, \\ \kappa &= T_2/T_1, P = (b/\alpha)(\Omega_0 - 1), \mu = k_{12} T_1/k_{11} b, \\ q_0 &= k_{11} b/r_1, k_{11} = \frac{1}{2}(d_{2332} - d_{3232}) \neq 0, \\ k_{12} &= \frac{1}{4} T^{-1} (\delta_{2323} - \delta_{3223} - \delta_{2332} + \delta_{3232}) \neq 0. \end{aligned} \quad (4.38)$$

In our problem, micropolar heat-conduction occurs only when k_{11} is not zero, for otherwise the problem will reduce to one of classical Fourier heat-conduction provided k_{12} does not vanish. There is an overwhelming experimental evidence¹⁰ to suggest that the thermal conductivity of nematic liquid crystal is anisotropic and that the classical heat-conduction law will not do in problems such as the one discussed in this paper. Hence, consistent with experimental evidence, we assume that k_{11} and k_{12} do not vanish.

The special nature of the boundary conditions on v , arrived above in (4.34), might appear strange at first sight. However, if we remember that the orientation field is heavily coupled with the boundary effects near the surface of the cylinders, we can readily recognize the fact that surface treatments and irregularities of the surface have drastic effects on the behavior of the gyration field near the surface. At present there seems to be no physical theory that can explain this interaction rationally. We must therefore revert to the experimental confirmation of our theory under the present boundary conditions on v . As will be discussed later the evidence appears to be gratifying on the basis of many new effects observed in experiments on nematic liquid crystals and the experimental verification of the present calculations are good.

5 ORIENTATION FIELD

It is clear from the remarks made at the end of the last section that one of the major questions yet unanswered is concerning the type of boundary conditions on orientation that prevails at a solid boundary in a given physical situation. One can expect a variety of possibilities for these boundary conditions as they are dependent on the prior treatment of the material of the boundary and also the type of the liquid crystals. Since the liquid crystals are composed of molecules which behave like dipole moments at a solid boundary, the answer to the above questions might lie in a thorough investigation of the distribution of electric charges at the boundary. Before discussing this any further, we shall first see what analytical expression could be obtained for the orientation field.

By integrating (4.14) and noting that n can only take the value unity in view of (4.26), and using (4.35), we have for the non-dimensional form of the orientation field:

$$\bar{\phi}(\lambda, \theta) = \frac{\lambda b}{\Omega_1} (\sigma \sin \theta - \cos \theta) + F_1(\lambda), \quad (5.1)$$

where $F_1(\lambda)$ is an arbitrary function of λ which can be determined with the help of the expression for the torque on the cylinders.

The torque per unit length about the z -axis on the cylinder of radius r , is denoted by τ and recalling that there is a contribution from the couple stress, we have

$$\tau = \int_0^{2\pi} (rm_{rz} + r^2 t_{r\theta}) d\theta. \quad (5.2)$$

By the use of our solutions (4.37) in the expressions (3.7) and (3.8) for the stress and couple stress components and substituting the resulting expressions for the latter into (5.2) we obtain

$$\frac{\tau}{2\pi B_{3131}} = \frac{1}{1 - R^2} [\gamma_1(1 - \Omega_0) + \lambda^2 \gamma_2(\Omega_0 - R^2)] + \lambda F'_1(\lambda), \quad (5.3)$$

where the prime denotes differentiation with respect to λ and where

$$\gamma_1 = -\frac{r_1^2 \Omega_1}{B_{3131}} (a_{1212} + a_{1221}), \gamma_2 = \frac{r_1^2 \Omega_1}{\alpha B_{3131}}. \quad (5.4)$$

Since the torque should remain the same on any cylinder of radius r , $r_1 \leq r \leq r_2$, as required by the balance of torques, we must have for all values of r , that is for λ , from (5.3),

$$F'_1(\lambda) = -\lambda \gamma_2 \left(\frac{\Omega_0 - R^2}{1 - R^2} \right), \quad (5.5)$$

which on integration yields the function

$$F_1(\lambda) = -\frac{1}{2}\lambda^2\gamma_2\left(\frac{\Omega_0 - R^2}{1 - R^2}\right) + K', \quad (5.6)$$

where K' is an arbitrary constant of integration. The expression for the torque, (5.3), after substituting for $F_1(\lambda)$ from (5.5) reduces to

$$\tau = 2\pi C, \quad (5.7)$$

where

$$C = \frac{r_1^2(a_{1212} + a_{1221})(\Omega_2 - \Omega_1)}{1 - R^2}, \quad (5.8)$$

is a constant representing the torque per unit length acting on the cylinders.

If we substitute (5.6) into (5.1), we find that the resulting expression for the orientation contains the arbitrary constant K' . Since the presence of a constant K' in the expression for the orientation does not affect the behavior of the orientation and its dependence on spatial coordinates λ and θ , the radius ratio R and the angular velocity ratio Ω_0 of the cylinders and furthermore K' does not appear in any of the solutions given by (4.37) or in the boundary conditions (4.16), (4.34) and (4.36), the arbitrary constant K' can as well be omitted. Hence we have finally the solution for the orientation field:

$$\bar{\phi}(\lambda, \theta) = \frac{\lambda b}{\Omega_1} (\sigma \sin \theta - \cos \theta) - \frac{1}{2}\lambda^2\gamma_2\left(\frac{\Omega_0 - R^2}{1 - R^2}\right). \quad (5.9)$$

We shall return to a discussion of the physical implication of this solution after obtaining the apparent viscosity which is a measure of the non-Newtonian behavior of the nematic liquid crystals.

6 APPARENT VISCOSITY

One can define an apparent viscosity such that it is equal to the constant coefficient of viscosity for the flow of an incompressible Newtonian fluid. Therefore, one can choose:

$$\eta_{\text{app}} = \left[\frac{\text{Shear stress}}{\text{Shear-rate on the outer cylinder}} \right]_{\text{at } \theta=0, \lambda=1/R}, \quad (6.1)$$

which becomes on using the known solutions for ω and v and also the expressions for shear-stress and shear rate:

$$\eta_{\text{app}} = a_{1212} + \frac{\Omega_2}{\gamma} (a_{1212} - a_{1221}) \left(1 - \frac{a}{\Omega_1 R} \right), \quad (6.2)$$

where the rate of shear γ is given by

$$\gamma = (r\omega')_{r=r_2} = \frac{2(\Omega_2 - \Omega_1)R^2}{1 - R^2}, \quad (6.3)$$

which is the uniform shear-rate at the outer cylinder. It is clear from (6.2) that

$$\eta_{\text{app}} = \hat{\eta}(\gamma, R). \quad (6.4)$$

First of all, we can study the limiting behavior of η_{app} when γ and R assume extreme values.

For narrow gap-width, using the approximation that the gap-width between the cylinders is very small compared to the mean radius, we have

$$r_2 - r_1 \ll \frac{1}{2}(r_1 + r_2),$$

or

$$D/D_0 \ll \frac{1}{2} < 1, \quad (6.5)$$

where

$$D = r_2 - r_1 \quad \text{and} \quad D_0 = r_2 + r_1.$$

On using (6.5), (6.2) reduces to:

$$\eta_{\text{app}} \underset{(R \text{ large})}{=} a_{1212} + \frac{\Omega_2}{\gamma} (a_{1212} - a_{1221}) \left[1 - \frac{a}{\Omega_1} \left(\frac{3 - R}{1 + R} \right) \right]. \quad (6.6)$$

For large gap-width, by using the approximation, $r_2 - r_1 \gg \frac{1}{2}(r_1 + r_2)$, (and this can be satisfied whenever $r_2 \gg 3r_1$), (6.2) becomes

$$\eta_{\text{app}} \underset{(R \text{ small})}{=} a_{1212} + \frac{\Omega_2}{\gamma} (a_{1212} - a_{1221}) \left[1 - \frac{a}{\Omega_1} \left(\frac{3R + 1}{1 - R} \right) \right]. \quad (6.7)$$

In like manner, for large shear rate $|\gamma|$, on using the approximation $|\Omega_2 - \Omega_1| \gg \frac{1}{2}|\Omega_1 + \Omega_2|$, (6.2) becomes:

$$\eta_{\text{app}} \underset{(|\gamma| \text{ large})}{=} a_{1212} + (a_{1212} - a_{1221})(\Omega_2 + a/R)/\gamma, \quad (6.8)$$

$$\eta_{\text{app}} \underset{(|\gamma| \rightarrow \infty)}{=} a_{1212} + (a_{1212} - a_{1221})(1 - R^2)/2R^2. \quad (6.9)$$

For small shear-rate $|\gamma|$, (here we assume that $|\gamma|$ has a non-zero lower bound which is not an unreasonable assumption in view of the usual experimental range of $|\gamma| = 60 \text{ sec}^{-1}$ to $18 \times 10^3 \text{ sec}^{-1}$), for cylinders rotating in the same sense, on using the approximation, $|\Omega_2 - \Omega_1| \ll |\Omega_1 + \Omega_2|$, we obtain

$$\lim_{|\gamma| \rightarrow \gamma_0 \neq 0 \text{ (small)}} \eta_{\text{app}} = a_{1212} + (a_{1212} - a_{1221})(\Omega_2 - a/R)/\gamma_0. \quad (6.10)$$

DISCUSSION AND COMPARISON WITH EXPERIMENTAL RESULTS

First of all, we notice that when we set the microgyration $\mathbf{v} = \mathbf{0}$ in our solutions (4.37) leading to the classical balance law of angular momentum, $t_{12} = t_{21}$, (which implies that $a_{1212} = a_{1221}$), our solutions are found to reduce to the well-known classical Newtonian viscous fluid flow solutions. Also, we have assumed in our solutions that $\Omega_1 \neq 0$, $a \neq 0$, $b \neq 0$, and $R \neq 1$, $B_{3131} \neq 0$, $a_{1212} - a_{1221} > 0$; the latter two conditions are permitted as discussed in Sect. 3, by the thermodynamic restrictions obtained in Ref. 5.

In the event $\Omega_1 = 0$ and $\Omega_2 \neq 0$, that is, the inner cylinder not rotating and the outer cylinder rotating, it follows from the boundary conditions (4.34) and the solutions (4.37) that both a and b should vanish in order to have a finite value for $v_2(\theta)$ which is found to be zero and $v_1(\theta)$ is also zero. Hence in this case (4.37), (5.4)₂, (5.9) and (6.2) yield the corresponding solutions:

$$\begin{aligned} \omega(r) &= \frac{\Omega_2 r_2^2}{r_2^2 - r_1^2} \left(1 - \frac{r_1^2}{r^2} \right), \quad v(r, \theta) = 0 = \phi(r, \theta), \quad p(r, \theta) = p(r_2, 0) \\ T(r) &= [(T_1 - T_2) \ln r + T_2 \ln r_1 - T_1 \ln r_2] / \ln R, \quad q_r = \frac{k_{12} T_1 (1 - \kappa)}{r \ln R} \\ q_\theta &= 0 = q_z, \quad \tau = 2\pi C = \frac{2\pi r_1^2 \Omega_2}{1 - R^2} (a_{1212} + a_{1221}), \end{aligned} \quad (7.1)$$

$$\eta_{app} = a_{1212} + \frac{\Omega_2}{\gamma} (a_{1212} - a_{1221}).$$

Next, when $\Omega_1 \neq 0$, $\Omega_2 = 0$, Eqs. (4.37), (5.4)₂, (5.8), (5.9) and (6.2) yield the following solutions:

$$\begin{aligned} \omega(r) &= \frac{\Omega_1 r_1^2}{r_2^2 - r_1^2} \left(\frac{r_2^2}{r^2} - 1 \right), \\ v(r, \theta) &= \frac{b r r_1}{r_2^2 - r_1^2} \left(\frac{r_2^2}{r^2} - 1 \right) (\sigma \cos \theta + \sin \theta), \\ p(r, \theta) - p(r_2, 0) &= \frac{1}{\alpha(1 - R^2)} \left[\frac{r}{r_1} \left(R + \frac{r_1^2}{r^2} \right) (\sigma \sin \theta - \cos \theta) + 2bR \right], \\ T(r) &= [(T_1 - T_2) \ln r + T_2 \ln r_1 - T_1 \ln r_2] / \ln R, \end{aligned} \quad (7.2)$$

$$\begin{aligned}
 q_r &= \frac{k_{11}b}{r_1(1-R^2)} \left(\frac{1}{\lambda^2} - R^2 \right) (\cos \theta - \sigma \sin \theta) \\
 &\quad + \frac{k_{12}T_1(1-\kappa)}{r \ln R}, \\
 q_\theta &= \frac{k_{11}b}{r_1(1-R^2)} \left(\frac{1}{\lambda^2} + R^2 \right) (\sigma \cos \theta + \sin \theta), \quad q_z = 0, \\
 \phi(r, \theta) &= \frac{\lambda b}{\Omega_1} (\sigma \sin \theta - \cos \theta) + \frac{1}{2} \lambda^2 \gamma_2 R^2 / (1 - R^2), \\
 \tau &= 2\pi C = -\frac{2\pi r_1^2 \Omega_1}{1 - R^2} (a_{1212} + a_{1221}), \quad \eta_{app} = a_{1212}.
 \end{aligned}$$

The case $\Omega_1 = 0 = \Omega_2$ is excluded from our problem since there is no shear-rate involved in that case. The case $R = 1$ is also excluded from our analysis since it reduces to the problem of a single tube rotating about its axis.

We are therefore interested in our investigation, primarily in the Couette flow between two concentric cylinders rotating in the same sense with distinctly different radii and angular velocities. Hence $\Omega_1 \neq \Omega_2$. Now, we shall discuss the behavior of the apparent viscosity.

From (6.2), (6.8) and (6.9), at a given temperature in the nematic range and for a fixed instrument the apparent viscosity is found to decrease as the shear-rate increases and when the shear-rate is above a certain value γ_c (which is determined later), the apparent viscosity levels off to a constant value given by (6.9). Also it follows from (6.2) and (6.10) that the apparent viscosity is found to depend strongly on the rate of shear at low shear-rates. At a given temperature in the nematic range, for a fixed radius-ratio, the apparent viscosity is found to increase rapidly as the shear-rate decreases, highest values of viscosity occurring at lowest possible values of shear-rate. The above predicted behavior of apparent viscosity is found to be in total agreement with the experimental results of Porter and Johnson,⁸ Peter and Peters,³³ and Miesowicz.³⁵ Furthermore, it is found from (6.6) to (6.10), that the limiting values of η_{app} for extreme values of the gap-width and rates of shear need not be the same. This also agrees with the experimental results stated above. Again, by comparing (6.2) with (6.6) and (6.7), higher values of apparent viscosity are found to occur for narrow gap-widths than those for arbitrary or finite gap-widths in the same range of shear-rate. This prediction from our theoretical results is also in good agreement with the above mentioned experimental results. Porter and Johnson,⁸ have attributed the higher values of the measured viscosity in narrow gap-width concentric rotating cylinder viscometers to another nonNewtonian behavior of the nematic mesophase, namely, the formation of very thin fluid layers called

adsorption layers adhering to the cylinder walls. We will now show that the experimental observation and the explanations offered by Porter and Johnson can be justified and confirmed by our theoretical results. According to Porter and Johnson,⁸ the increase in viscosity above the precision limits is due to the fluid adhering to the cylinder walls, thus resulting in an effective decrease in fluid thickness. Apart from these adsorption layers at the cylinder walls, the remainder of the liquid crystal flows with its uniform high shear viscosity as in the case of finite or large gap-widths. These adsorption layers are so thin that they influence the measurement of viscosity only in the case of very small gap-widths.

Now, since a fluid layer is formed at the walls, one can introduce an adsorption layer thickness δ defining it in a natural way as follows. First of all, it is easy to observe from Eqs. (6.6) and (6.8) that both the limiting viscosities reduce to the effective viscosity for very high shear-rates and this value is found to be a_{1212} . Using this effective viscosity in our formula for the torque, Eq. (5.8), we can define the adsorption layer thickness δ , which is essentially the difference between the apparent gap-width and the real gap-width of the Couette instrument, as follows:

$$C = 2(\Omega_2 - \Omega_1)a_{1212} \left\{ \left(\frac{1}{r_1 + \delta} \right)^2 - \left(\frac{1}{r_2 - \delta} \right)^2 \right\}^{-1}. \quad (7.3)$$

Applying the narrow gap-width approximation (6.5) on (7.3), we obtain the non-dimensional adsorption layer thickness $\delta^* = \delta/r_2$ given by

$$\delta^* = \frac{\delta}{r_2} = \frac{1}{2} \left| (1 - R) - (3R - 1) \left(\frac{\Omega_2 - \Omega_1}{\gamma} \right) \left(\frac{a_{1212}}{a_{1212} + a_{1221}} \right) \right| \quad (7.4)$$

which clearly, is found to vanish in the narrow gap-width case for a Newtonian fluid, ($a_{1212} = a_{1221}$), since, in view of (6.5) and (6.3), we have the approximations, $1 - R \simeq 2D/D_0$, $1 - R^2 \simeq 4D/D_0$ and $(\Omega_2 - \Omega_1)/\gamma \simeq 2D/D_0$, which when substituted in (7.4) yield $\delta^* = 0$.

We will now show that our theoretical results are in very close qualitative as well as quantitative agreement with the experimental results of Porter and Johnson,⁸ Peter and Peters,³³ Becherer and Kast³⁴ and Miesowicz³⁵ involving a typical nematic mesophase, *p*-azoxyanisole. But before this, we will demonstrate the method of determining the material coefficients present in our constitutive equations for the case of *p*-azoxyanisole with the help of the experimental data. The general range of shear-rates considered by the above experimentalists is from about 60 sec^{-1} to $18 \times 10^3 \text{ sec}^{-1}$, and the nematic temperature range for *p*-azoxyanisole is from about 119°C to about 135°C , where 119°C is approximately the transition temperature

at which the solid nematic and nematic liquid-crystalline states are in equilibrium. The upper limit 135°C is approximately the temperature at which nematic-isotropic transition occurs. Above 135°C we have the isotropic case.

In order to determine the material coefficients a_{1212} and a_{1221} involved in our result (6.2), we need two equations, one of which can be obtained by equating the limiting value of η_{app} given by (6.9) for very high shear-rates $\gamma \sim 18 \times 10^3 \text{ sec}^{-1}$, at a given temperature to the experimentally observed limiting orientational viscosities calculated from the graphs of Porter and Johnson,⁸ and Peter and Peters.³³ The second equation is obtained by equating the adsorption layer thickness given by (7.4) to the experimental values computed from the graphs of Porter and Johnson.⁸ a_{1212} and a_{1221} are then determined by solving the resulting two equations.

Experimental data from Peter and Peters:³³

Diameters of the inner and outer cylinders are, respectively, 3.96 cm and 4.00 cm. Lengths of the two cylinders are 14 cm and 20 cm respectively, so that the end effects may be neglected. Table 1 below gives the experimental values of limiting η_{app} for high shear-rates,

TABLE 1

Temperature ($^{\circ}\text{C}$)	Limiting $\eta_{\text{app}} = L_{\eta}$ (in centipoise)
119	2.59
122	2.51
125	2.45
128	2.40
131	2.36

Substituting the value of $R = 0.99$ into (6.9) and equating the result to L_{η} given in Table 1, we obtain

$$1.01a_{1212} - 0.01a_{1221} = L_{\eta} \quad (7.5)$$

We compute the values of the adsorption layer thickness δ from the experimental graphs of Porter and Johnson. For instance, at 128°C , for fluid thickness, $r_2 - r_1 = 3.35 \times 10^{-4} \text{ cm}$, the value of $2\delta = 0.6 \times 10^{-4} \text{ cm}$. Choosing for convenience the inner cylinder radius r_1 as the standard unit, that is, $r_1 = 1$, we have then $R \simeq 1 - 3.95 \times 10^{-4}$. For $\gamma \sim 10^3 \text{ sec}^{-1}$, we have from (7.4) on substituting $\delta = 0.3 \times 10^{-4} \text{ cm}$, at 128°C ,

$$a_{1212} = 1.3581a_{1221}. \quad (7.6)$$

We remark here that because of the very small values of the adsorption layer thickness δ (about $0.3 \times 10^{-4} \text{ cm}$), Eq. (7.6) is found to hold with

notable constancy for the entire nematic temperature range up to about 135°C, without any appreciable modification. Now, from (7.5) and (7.6) and Table 1, we obtain the values of a_{1212} and a_{1221} given in Table 2.

TABLE 2

Temperature (°C)	a_{1212} in centipoise	a_{1221} in centipoise
119	2.583	1.902
122	2.503	1.844
125	2.443	1.799
128	2.393	1.762
131	2.354	1.733

An estimate of the material coefficient B_{3131} present in our constitutive theory, can be obtained by a comparison of our theory with the experimental work of Saupe³⁷ who, assuming the static theory of Frank²⁶ to be valid for *p*-azoxyanisole has determined the values of the Frank's constants to be of the order of 10^{-6} dyn. The Frank's constants correspond to the material coefficients B_{klmn} present in our theory, since Frank's relations

$$G = \int_V \rho g \, dV, \quad \rho g = k_i a_i + \frac{1}{2} k_{\alpha\beta\gamma\delta} a_{\alpha\beta} a_{\gamma\delta}, \quad \rho \frac{\partial^2 g}{\partial a_{\alpha\beta} \partial a_{\gamma\delta}} = k_{\alpha\beta\gamma\delta},$$

$$i, j = 1, 2, 3, \dots, 6; \quad k_{\alpha\beta\gamma\delta} = k_{\gamma\delta\alpha\beta}. \quad (7.7)$$

where G = total free energy, ρg = free energy density per unit volume, $a_{\alpha\beta}$ = curvature-strain components, correspond to Eringen-Lee theory¹²⁻¹⁴ and also our theory,⁵ in the linear case, namely,

$$\rho \frac{\partial^2 \psi}{\partial \phi_{k,l} \partial \phi_{m,n}} = B_{klmn}, \quad (7.8)$$

where ψ = free energy density per unit mass and $\phi_{k,l}$ = orientational gradient. The comparison of (7.7) and (7.8) at once leads to the conclusion that the Frank's constants $k_{\alpha\beta\gamma\delta}$ coincide with B_{klmn} of the present theory. Hence it follows that

$$B_{3131} \simeq 10^{-6} \text{ dyn.} \quad (7.9)$$

In order to determine the nature of the term $[1 - (a/\Omega_1 R)]$ in (6.2), we revert back to the discussion of the orientation field. In Sect. 5, we have mentioned that the boundary conditions on orientation are at present unknown and they depend on the nature of the liquid crystal and also prior treatment of the material of the boundary (see Brown and Shaw³⁸). For instance, Fisher and Fredrickson,³⁹ following the suggestion of J. Ferguson of the liquid crystal institute (Kent, Ohio), have used in their experiments

certain techniques to obtain very nearly the desired orientation at the boundary. They find that a bundle of human hairs when rubbed to-and-fro about 150 times on the boundary can produce parallel orientation. In order to obtain perpendicular orientation of *p*-azoxyanisole the boundary needs to be washed in sulfuric acid-dichromate solution for about twenty minutes, rinsed with distilled water and dried with air, while the tubes are immersed in hot oil constant temperature. Other boundary conditions are possible. In order to fix ideas, for instance, if we have perpendicular orientation at both the boundaries $r = r_1$ and $r = r_2$, i.e., $\lambda = 1$ and $\lambda = 1/R$, then in particular, we should have

$$\bar{\phi}\left(\frac{1}{R}, \frac{\pi}{2}\right) = -\frac{\pi}{2} = \bar{\phi}\left(1, \frac{\pi}{2}\right), \quad (7.10)$$

where the X -axis of the material frame is chosen to coincide with the axis of orientation as mentioned before, and the angle of orientation is measured as the angle which the axis of orientation makes with the long axis of a single molecule. From (7.10) we have

$$\bar{\phi}\left(1, \frac{\pi}{2}\right) - R^2 \bar{\phi}\left(\frac{1}{R}, \frac{\pi}{2}\right) = -\frac{\pi}{2}(1 - R^2),$$

which on using (5.9) and solving for a/Ω_1 yields

$$\frac{a}{\Omega_1} = -\frac{\pi}{2}(1 + R),$$

and hence we obtain

$$1 - \frac{a}{\Omega_1 R} = 1 + \frac{\pi}{2}\left(1 + \frac{1}{R}\right). \quad (7.11)$$

It is easy to find that $\bar{\phi}(\lambda, \theta)$ possesses a maximum $\bar{\phi}_m$ at the interior point (λ_1, θ_1) of the domain $\lambda \in [1, 1/R]$ and $\theta \in [0, 2\pi]$, where

$$\lambda_1 = \frac{K\Delta B_{3131}}{C + K}, \theta_1 = \pi - \theta_m, \theta_m = \tan^{-1}(a/b), \quad (7.12)$$

$$K = r_1^2 \Omega_1 (a_{1212} + a_{1221}), C = \frac{\tau}{2\pi} = \frac{K(\Omega_0 - 1)}{1 - R^2}, \quad (7.13)$$

$$\Delta = \alpha(a^2 + b^2)^{1/2}/r_1^2 \Omega_1^2 > 0,$$

provided the following inequalities are satisfied:

$$(C + K)/K > 0, 1 < K\Delta B_{3131}/(C + K) < 1/R. \quad (7.14)$$

The maximum orientation ϕ_m is then given by

$$\bar{\phi}_m = \beta(a^2 + b^2) \left(\frac{B_{3131}}{C + K} \right), \quad (7.15)$$

where

$$\beta = \frac{1}{2}(a_{1212} + a_{1221})/(a_{1212} - a_{1221}) > 0. \quad (7.16)$$

In view of (7.14) and (7.15), it follows that the maximum orientation can be made to occur arbitrarily close to the inner or outer cylinder wall by choosing the torque C sufficiently close to $K(\Delta B_{3131} - 1)$ or to $K(\Delta R B_{3131} - 1)$, respectively. This implies that the walls significantly influence the orientation only when $K\Delta B_{3131}/(C + K)$ is of the order of unity or greater, that is, when

$$|C + K| < |K|\Delta B_{3131}. \quad (7.17)$$

Since from (7.9), $B_{3131} \simeq 10^{-6}$ dyn and positive, we find from (7.17) that the walls significantly influence the orientation only when $|C| \simeq 10^{-6}$ dyn or less; otherwise the flow dictates the orientation except in the adsorption layers at the walls. This result agrees with the conclusions of Atkin and Leslie.³¹

Once again, in order to fix ideas, for instance, if we have perpendicular orientation at both the boundaries, after using (7.10) in (5.9) and solving for $C + K$ and substituting its value into (7.14), we find that the latter inequality reduces to

$$2\pi\beta R/\Delta < -K < 2\pi\beta/\Delta. \quad (7.18)$$

(7.18) suggests that in the case of perpendicular orientation at both the boundaries, we must have, since both $\Delta > 0$ and $\beta > 0$,

$$K < 0, \quad (7.19)$$

and in view of (7.14)₁ we must have also,

$$C + K < 0.$$

(7.19) implies on account of (7.13)_{1,2}, that $\Omega_1 < 0$ and $\Omega_2 < 0$, which means that the cylinders are rotating in the same sense as assumed earlier. For convenience, we shall regard the inner cylinder as rotating with a fixed angular velocity Ω_1 and the shear-rate variation can then be effected by varying the magnitude of the angular velocity Ω_2 of the outer cylinder. Once again, from the experimental data of Peter and Peters,³³ we obtain by using (7.11) and (6.3), since $R = 0.99$,

$$1 - \frac{a}{\Omega_1 R} = 4.158, \quad \frac{\Omega_2}{\gamma} = 0.01 + \frac{\Omega_1}{\gamma} \quad (7.20)$$

Since Ω_1 is regarded as fixed and negative, while Ω_2 is negative and is varied continuously assuming all possible values within the experimental range, and for large $|\gamma|$, Ω_2 has to be large, it will be sufficient if we consider the cases for which $\Omega_2 - \Omega_1 < 0$, that is, for which $\gamma < 0$. Choosing $|\Omega_1| = 11.84$ radians per second, with the aid of the experiments, we have from $(7.20)_2$, since $\Omega_2/\gamma > 0$,

$$\frac{\Omega_2}{\gamma} = 0.01 + \frac{11.84}{|\gamma|}. \quad (7.21)$$

Substituting (7.21) and $(7.20)_1$ in (6.2), we obtain for the nematic *p*-azoxy-anisole:

$$\eta_{app} = a_{1212} + (4.158) \left(0.01 + \frac{11.84}{|\gamma|} \right) (a_{1212} - a_{1221}). \quad (7.22)$$

Now we compute the apparent viscosity η_{app} from (7.22) for the nematic *p*-azoxyanisole within its nematic temperature range 119°C to 135°C and shear-rate range 60 sec^{-1} to $18 \times 10^3 \text{ sec}^{-1}$, using the known values of a_{1212} and a_{1221} from Table 2. The theoretical curves obtained are shown in Figure 1, apparent viscosity versus shear-rates at various nematic temper-

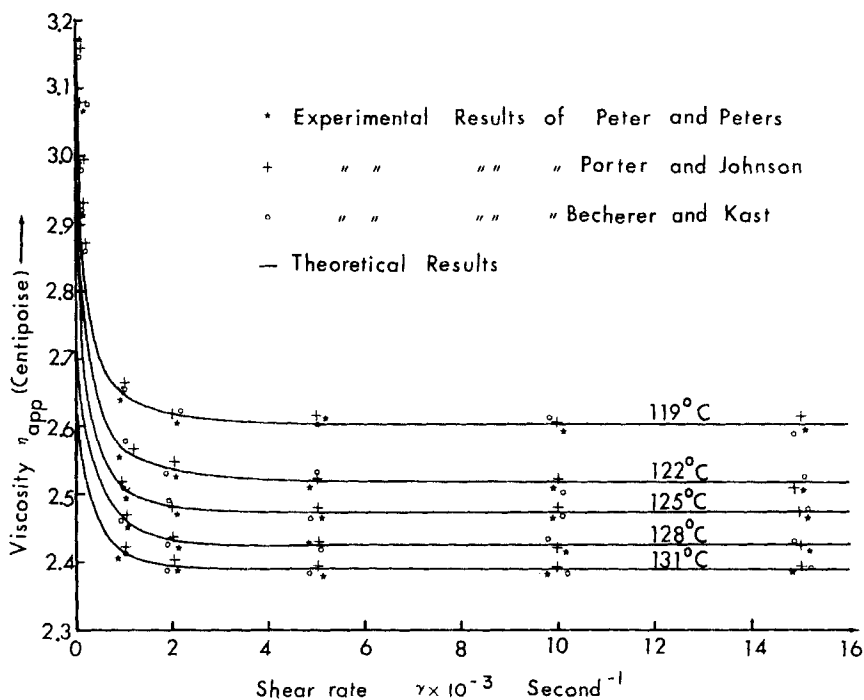


FIGURE 1 Behavior of apparent viscosity with shear-rate

atures. In the same Figure 1, for purposes of comparison with experimental results, we have also plotted the corresponding values of the apparent viscosity calculated from three sets of experimental curves, those of Porter and Johnson,⁸ Peter and Peters³³ and Becherer and Kast³⁴ at each nematic temperature and shear-rate value. From Figure 1, it is found that viscosities for the nematic state are found to increase if shear-rate is decreased below a homogeneous value of about 2000 sec^{-1} , and above this value of the shear-rate, the viscosity is found to level off to a constant value, at each value of the nematic temperature. The theoretical values of apparent viscosity obtained in our work are found to be in close qualitative as well as quantitative agreement with the experimental results. In order to further elucidate the strong shear-rate dependence of the viscosity at low values of the rate of shear, Figure 2 is drawn to contain the plot of η_{app} versus the reciprocal of the shear-rate, namely, $G = 1/|\dot{\gamma}|$ and reveals the strong non-Newtonian character of the nematic liquid crystal at low shear-rates. These results are in good agreement with the experimental results mentioned above. For instance, our theoretically predicted value of 3.17 centipoise for viscosity of *p*-azoxyanisole at a temperature of 119°C and shear-rate equal to 60 sec^{-1} , agrees with the experimental value of 3.17 centipoise reported by Peter and Peters³³ at shear-rate equal to about 58 sec^{-1} and at temperature 119°C and again from Figure 2, the high viscosity value of 9.27 centipoise predicted by our theory for perpendicular orientation at the boundaries, at low rates of shear agrees very closely with the experimental value of 9.2 centipoise obtained by Miesowicz³⁵ under similar conditions.

We now turn to the discussion of heat-conduction effects versus shear-effects on orientation. In Eqs. (4.37)_{5,6} for heat-conduction, it is clear that the first terms are contributions from microgyration and the second term in (4.37)₅ is the contribution from the externally imposed temperature gradient. Hence it follows that heat-conduction can occur in micropolar flow even in the absence of an externally imposed temperature gradient.

It follows from (4.37)₅ that the expression for the orientation field (5.9) can be rewritten in the form

$$\bar{\phi}(\lambda, \theta) = \bar{Q}_\lambda + \bar{\tau}_\lambda, \quad (7.23)$$

where \bar{Q}_λ and $\bar{\tau}_\lambda$ are, respectively, the contributions to orientation from heat-conduction and shear and are given by

$$\bar{Q}_\lambda = - \left[\bar{q}_\lambda - \frac{\mu(1-\kappa)}{\lambda \ln R} \right] / \left[1 + \frac{C}{K} \left(1 - \frac{1}{\lambda^2} \right) \right], \quad (7.24)$$

$$\bar{\tau}_\lambda = - \frac{1}{2} \frac{\lambda r_1^2 \Omega_1}{\alpha B_{3131}} \left(1 + \frac{C}{K} \right). \quad (7.25)$$

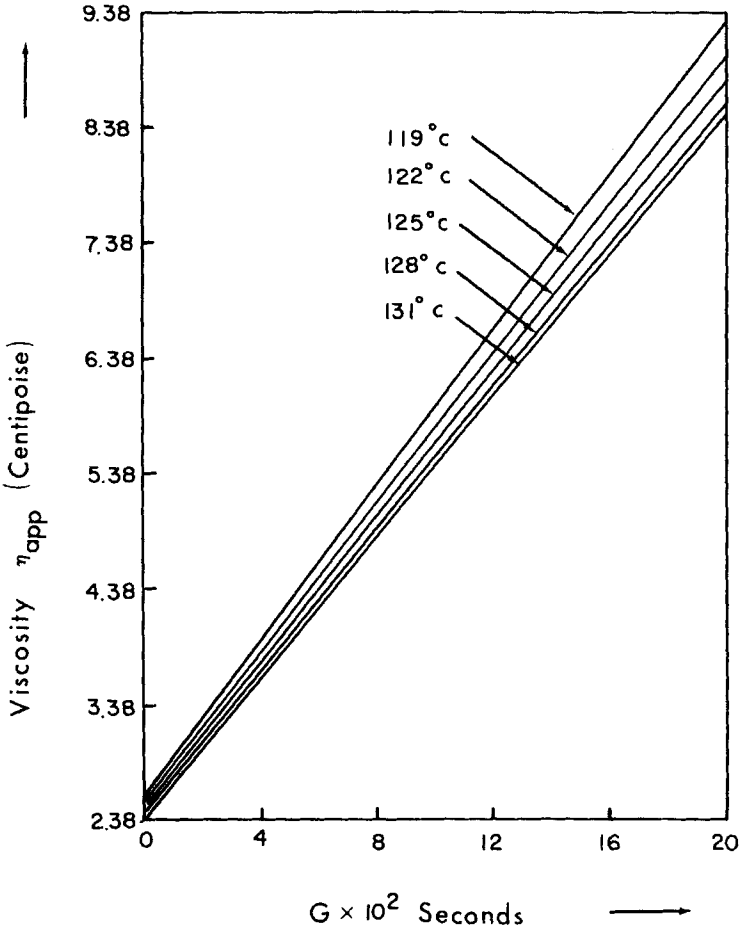


FIGURE 2 Apparent viscosity versus reciprocal shear-rate

Using (4.37)₅, the relative order of magnitude of \bar{Q}_λ and $\bar{\tau}_\lambda$ becomes

$$\bar{Q}_\lambda/\bar{\tau}_\lambda = \frac{-2b(\sigma \sin \theta - \cos \theta)\alpha B_{3131}}{\lambda r_1^2 \Omega_1^2 \left(1 + \frac{C}{K}\right)} \tag{7.26}$$

Replacing, on the right-hand side of (7.26), λ by its minimum value unity, and $(\sigma \sin \theta - \cos \theta)$ by its maximum value $\sigma \sin \theta_1 - \cos \theta_1 = (a^2 + b^2)^{1/2}/b$, from (7.12), we obtain after using (7.13)₃,

$$\bar{Q}_\lambda/\bar{\tau}_\lambda \leq \left| \frac{-2\Delta K B_{3131}}{C + K} \right|, \tag{7.27}$$

Since, from (7.14)₂, we have $K\Delta B_{3131}/(C + K) > 0$, (7.27) can be rewritten as

$$\bar{Q}_\lambda/\bar{\tau}_\lambda \leq \frac{2\Delta KB_{3131}}{C + K} = \frac{2\Delta B_{3131}}{1 + C/K} \leq \frac{2\Delta B_{3131}}{C/K}. \quad (7.28)$$

From (7.28), it follows that the heat-conduction effects on orientation of the nematic mesophase do not compete successfully with shear-effects unless the torque C is below a certain value C_1 which is estimated below for p -azoxy-anisole.

At a given temperature say 128°C, from our Table 2, we have

$$\begin{aligned} \alpha &= (a_{1212} - a_{1221})^{-1} = 1.585 \text{ (centipoise)}^{-1}, |K| = |r_1^2 \Omega_1 (a_{1212} + a_{1221})| \\ &= 142.9 \text{ dyne}, \\ r_1^2 &= 3.921, \Omega_1^2 = 140.3, \frac{a}{\Omega_1} = -3.127, \frac{b}{\Omega_1} = -6.254, \end{aligned} \quad (7.29)$$

$$\Delta = \alpha(a^2 + b^2)^{1/2}/r_1^2 \Omega_1^2 = 2.828,$$

(here we have chosen $b = 2a$).

Since $B_{3131} \simeq 10^{-6}$ dyn from (7.9), we find from (7.28) on using the data (7.29) that the heat-conduction effects on orientation are much smaller than

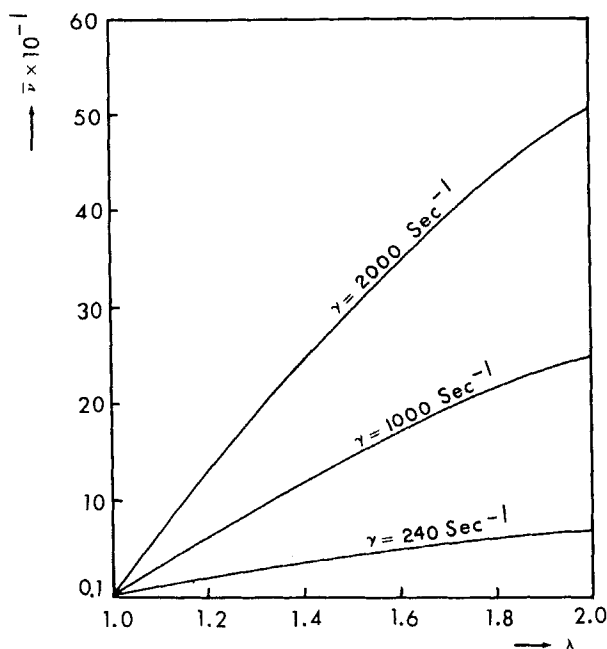


FIGURE 3 Microgyration velocity versus radial distance ($\theta = 0.5\pi$)

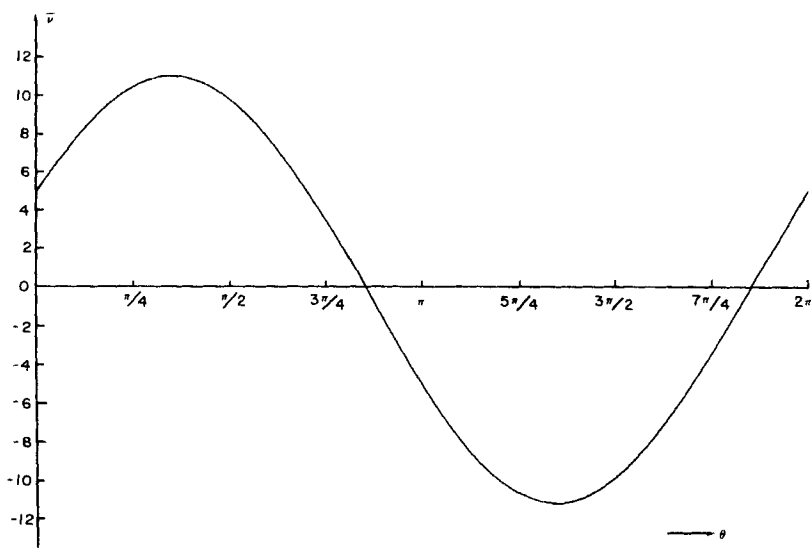


FIGURE 4 Microgyration velocity versus polar angle ($\lambda = 1.5$, $\gamma = 60 \text{ sec}^{-1}$)

the shear orientation-effects unless $|C| \leq 10^{-3}$ dyn. Hence, heat-conduction does not affect orientation appreciably at torques above 10^{-3} dyn, a result which agrees with the experimental conclusions of Porter and Johnson⁸ and Picot and Fredrickson.¹⁰

Figures 3 and 4 depict the microgyration behavior under varying rates of shear throughout the annulus of the rotating viscometer. It is found from Figure 3, that for a fixed instrument and for a given angle θ , ($R = 1/2$, $\theta = \pi/2$), the gyration field increases with the radial distance and this increasing trend becomes more pronounced with higher rates of shear as is to be expected on physical grounds. Figure 4 gives the variation of the gyration field with the angular coordinate θ , for a fixed instrument, at a given radial distance λ and for a given shear-rate ($R = 1/2$, $\sigma = 1/2$, $\lambda = 1.5$, $\gamma = 60 \text{ sec}^{-1}$). The oscillatory behavior of the gyration field as a function of θ is clearly the consequence of the type of the boundary conditions considered for the gyration field in our problem.

References

1. A. C. Eringen and E. S. Suhubi, "Non-linear theory of simple microelastic solids—I," *Int. J. Eng. Sci.*, **2**, 189 (1964).
2. A. C. Eringen, "Simple microfluids," *Int. J. Eng. Sci.*, **2**, 205 (1964).
3. A. C. Eringen, "Theory of micropolar fluids," *J. Math. Mech.*, **16**, 1 (1966).
4. A. C. Eringen, "Linear theory of micropolar elasticity," *J. Math. Mech.*, **15**, 909 (1966).
5. M. N. L. Narasimhan and A. C. Eringen, "Thermomicropolar theory of heat-conducting nematic liquid crystals", appearing in *Int. J. Eng. Sci.*

6. G. H. Heilmeyer, *J. Chem. Phys.*, **44**, 644 (1966).
7. H. Zocher, *Trans. Faraday Soc.*, **29**, 945 (1933).
8. R. S. Porter and J. F. Johnson, "Orientation of nematic mesophases", *J. Phys. Chem.*, **66**, 1826 (1962).
9. R. S. Porter, E. M. Barrall, II, and J. F. Johnson, *J. Chem. Phys.*, **45**, 1452 (1966).
10. J. J. C. Picot and A. G. Fredrickson, "Interfacial tension and electrical effects on thermal conductivity of nematic liquid crystals", *Ind. Eng. Chem. Fundamentals* (1), **7**, 84 (1968).
11. P. Chatelain, *Compt. Rend.*, **213**, 875 (1941).
12. J. D. Lee and A. C. Eringen, "Boundary orientation effects of nematic liquid crystals", *J. Chem. Phys.* (9), **55**, 4509 (1971).
13. J. D. Lee and A. C. Eringen, "Wave propagation in nematic liquid crystals", *J. Chem. Phys.* (12), **54**, 5027 (1971).
14. J. D. Lee and A. C. Eringen, "Alignment of nematic liquid crystals", *J. Chem. Phys.*, **55**, 4504 (1971).
15. O. Lehmann, "Structur. System und Magnetisches Verhalten Flussiger Krystelle und deren Mischbarkeit mit festen", *Ann. Phys.* (4), **2**, 649 (1900).
16. A. Anzelius, *Uppsala Univ. Årsskr. Mat. Och Naturvet*, **1**, (1931).
17. C. W. Oseen, "The theory of liquid crystals", *Trans. Faraday Soc.*, **29**, 883 (1933).
18. F. M. Leslie, "Some thermal effects in cholesteric liquid crystals", *Proc. Roy. Soc.*, **A307**, 359 (1968).
19. F. M. Leslie, "Some constitutive equations for liquid crystals", *Arch. Ratl. Mech. Anal.*, **28**, 265 (1968).
20. V. S. V. Rajan and J. J. C. Picot, "Thermal transport phenomena in nematic liquid crystals: A Review", *Mol. Cryst. Liq. Cryst.*, **20**, 55 (1973).
21. F. M. Leslie, "Continuum theory of thermotropic systems" (general discussions), *Sym. Liq. Cryst.*, Faraday Society, London, 1971.
22. G. W. Stewart, *J. Chem. Phys.*, **4**, 231 (1936).
23. C. K. Yun, et al., *J. Appl. Phys.*, **42**, 4764 (1971).
24. J. A. Fisher and A. G. Fredrickson, *Mol. Cryst. Liq. Cryst.*, **6**, 255 (1969).
25. G. W. Stewart, D. O. Holland, and L. M. Reynolds, "Orientation of liquid crystals by heat conduction", *Phys. Rev.*, **58**, 174 (1940).
26. L. Davison, "Linear theory of heat-conduction and dissipation in liquid crystals of the nematic type", *Phys. Rev.*, **180**, 232 (1969).
27. L. Davison and D. E. Amos, "Dissipation in liquid crystals", *Phys. Rev.*, **183**, 288 (1969).
28. J. L. Ericksen, "Conservation laws for liquid crystals", *Trans. Soc. Rheology*, **5**, 23 (1961).
29. J. L. Ericksen, "Hydrostatic theory of liquid crystals", *Arch. Ratl. Mech. Anal.*, **9**, 371 (1962).
30. A. C. Eringen, *Proc. of the Eleventh Int. Congr. of Appl. Mech., Munich, Germany*, Ed. H. Görtler (Springer, Berlin), 131 (1964).
31. R. J. Atkin and F. M. Leslie, "Couette flow of nematic liquid crystals" *Quart. J. Mech. and Appl. Math.*, **23**, Part 2, S3 (1970).
32. R. J. Atkin, "Poiseuille flow of liquid crystals of the nematic type", *Arch. Ratl. Mech. and Anal.* (3), **38**, 224 (1970).
33. S. Peter and H. Peters, *Zeit. für Physik. Chemie.*, **3**, S103 (1955).
34. G. Becherer and W. Kast, *Ann. Phys.*, **41**, 355 (1942).
35. M. Miesowicz, "The three coefficients of viscosity of anisotropic liquids", *Nature*, **158**, 27 (1946).
36. F. C. Frank, *Discuss. Faraday Soc.*, **25**, 19 (1958).
37. A. Saupe, *Z. Naturf.*, **15A**, 815 (1960).
38. G. H. Brown and W. H. Shaw, *Chem. Rev.*, **57**, 1049 (1957).
39. J. Fisher and A. G. Fredrickson, "Interfacial effects on the viscosity of a nematic mesophase", *Mol. Cryst. Liq. Cryst.*, **8**, 267 (1969).
40. A. C. Eringen, *Fracture*, edited by H. Liebowitz (Academic Press, New York), Vol. 2, (1968), p. 681.